Femtosecond Broadband Stimulated Raman Spectroscopy

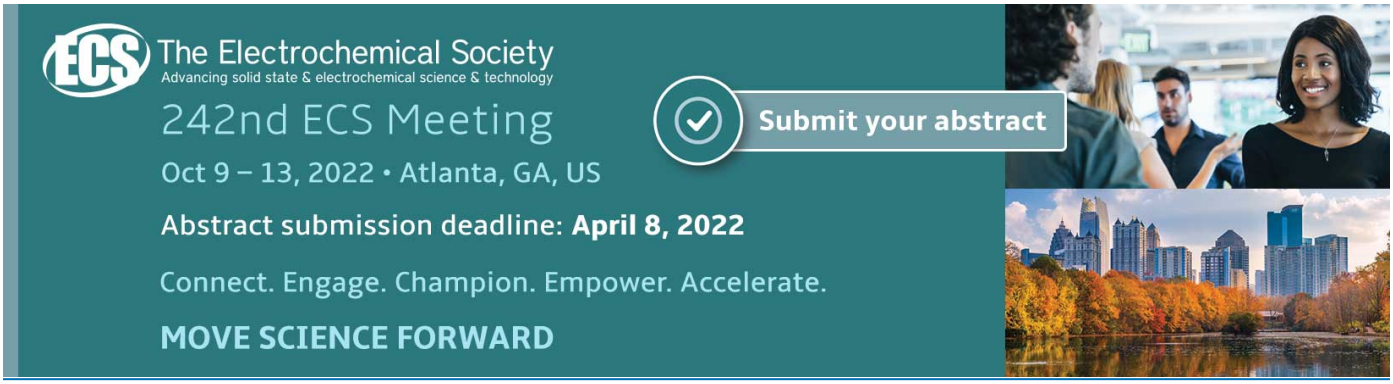

Institute of Physics Publishing Journal of Physics: Conference Series **28** (2006) 36–41
doi:10.1088/1742-6596/28/1/007 International Conference on Materials for Advanced Technologies, Symposium Y

Femtosecond Broadband Stimulated Raman Spectroscopy

Soo-Y. Lee[1,a], Sangwoon Yoon[2] and Richard A. Mathies[2]

[1]School of Physical & Mathematical Sciences, Nanyang Technological University, 1 Nanyang Walk, Singapore 637616
[2]Department of Chemistry, University of California, Berkeley, California 94720, USA

[a]E-mail: sooying@ntu.edu.sg

Abstract. Femtosecond broadband stimulated Raman spectroscopy (FSRS) is a new technique where a narrow bandwidth picosecond Raman pump pulse and a red-shifted broadband femtosecond Stokes probe pulse (with or without time delay between the pulses) act on a sample to produce a high resolution Raman gain spectrum with high efficiency and speed, free from fluorescence background interference. It can reveal vibrational structural information and dynamics of stationary or transient states. Here, the quantum picture for femtosecond broadband stimulated Raman spectroscopy (FSRS) is used to develop the semiclassical coupled wave theory of the phenomenon and to derive an expression for the measurable Raman gain in FSRS. The semiclassical theory is applied to study the dependence of lineshapes in FSRS on the pump-probe time delay and to deduce vibrational dephasing times in cyclohexane in the ground state.

1. Introduction

Femtosecond broadband stimulated Raman spectroscopy (FSRS) is a new technique that can reveal vibrational structural information of stationary or transient states [1-4]. In FSRS, a narrow bandwidth picosecond Raman pump pulse and a broadband femtosecond Stokes probe pulse to the red of the pump (with or without time delay between the pulses) act on the sample to produce a high resolution Raman gain spectrum with high efficiency and speed, free from fluorescence background interference. When FSRS is preceded by an ultrafast laser pulse that prepares the molecule in an excited electronic state, time-resolved studies can be carried out to explore the evolution of the vibrational structure of transient species with both high temporal (< 100 fs) and spectral (~10 cm^{-1}) resolution, overcoming the pulse duration/bandwidth transform limit in conventional time-resolved Raman spectroscopy. The FSRS has been used to study the excited electronic state dynamics of polyenes and of biological pigments.

Early classical and quantum theories for stimulated Raman scattering were developed for cw fields [5], which clearly had to be modified and extended to pulsed fields for FSRS. Lee *et al.* [6-7] developed both semiclassical coupled wave and quantum mechanical approaches for FSRS, and showed the correspondence between the two approaches under the following principal assumptions: (a) the Raman pump frequency is off-resonant with any excited electronic state, and (b) the molecule undergoes a fundamental Stokes Raman transition. Here we present an intuitive connection between the quantum and semiclassical approaches to FSRS and derive the result for the Raman gain. The dependence of lineshapes on pump-probe delay time and the deduction of vibrational dephasing times are illustrated with cyclohexane in the ground state.

2. Theory

The quantum mechanical description of (off-resonant) FSRS using the energy ladder, bra-ket time evolution diagram of Lee and Albrecht [8] is shown in figure 1.

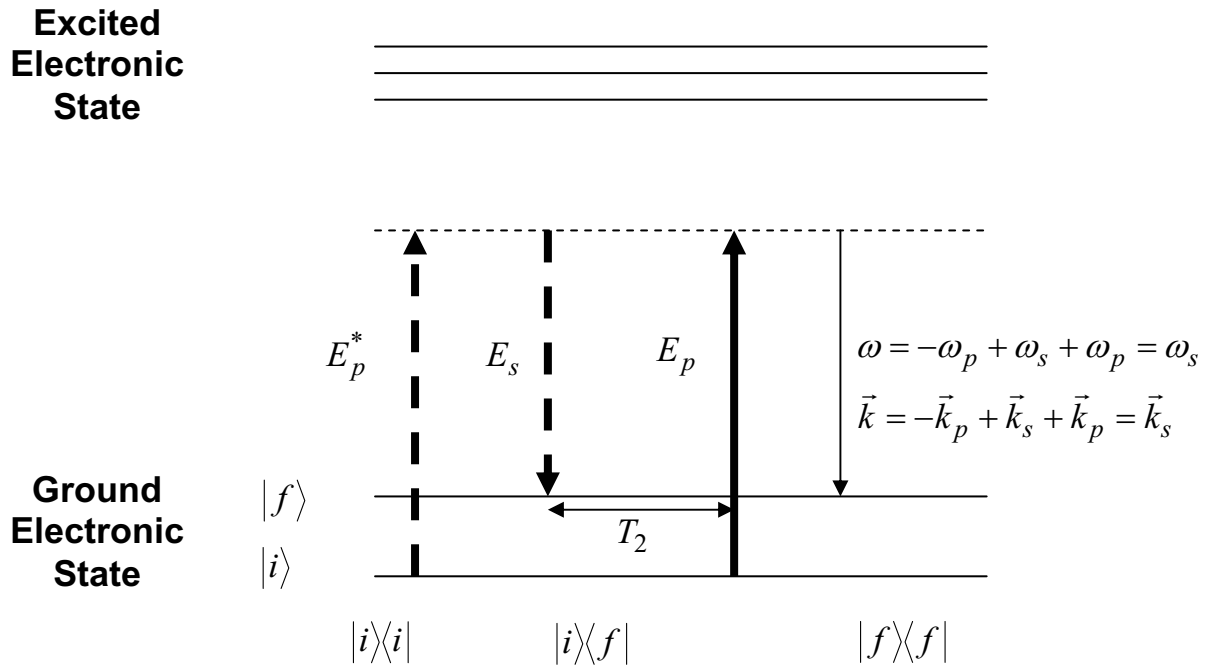

Figure 1. Wave mixing energy level diagram in Liouville space for FSRS.

The first two up and down dashed arrows correspond to the Raman pump field E_p^* coupled with a Stokes probe field E_s, respectively, interacting with the bra $\langle i|$ and exciting it to a bra $\langle f|$, and the system changes from an initial Liouville state $|i\rangle\langle i|$ to the state $|i\rangle\langle f|$. The resulting resonant second-order density matrix element $\rho_{fi}^{(2)*}(\omega_p - \omega_s)$ has equation of motion,

$$\left(\frac{\partial}{\partial t} - i\omega_0 + \gamma\right)\rho_{fi}^{(2)*}(\omega_p - \omega_s) = -\frac{i}{\hbar}\alpha_{fi}^* E_p^* E_s(\rho_i - \rho_f) \ , \tag{1}$$

where $\omega_0 \equiv \omega_{fi}$, $\gamma = T_2^{-1}$, α_{fi} is the polarizability element, and ρ_i, ρ_f are the populations in states *i*, *f*, respectively. Here we assume that $\rho_i = 1$ and $\rho_f = 0$. It is conventional to identify $\rho_{fi}^{(2)}(\omega)$ with $(\hbar/2\omega)^{-1/2}Q$, where Q is a normal coordinate. With the resonance condition $\omega_p - \omega_s \approx \omega_0$ and $\gamma << \omega_0$ it can be shown that equation (1) is equivalent to that for a driven harmonic oscillator

$$\left(\frac{\partial^2}{\partial t^2} + 2\gamma\frac{\partial}{\partial t} + \omega_0^2\right)Q^* = \left[\frac{2(\omega_p - \omega_s)}{\hbar}\right]^{1/2}\alpha_{fi}^* E_p^* E_s \ . \tag{2}$$

The coupled fields E_p^*, E_s can be said to create a coherent vibration *Q(t)* in the system. In the Placzek polarizability model, the change in polarization in the medium arises from the interaction of $Q^*(t)$ with the (long) Raman pump field E_p, designated by the solid up arrow acting on the ket $|i\rangle$. The polarized medium then radiates, and energy conservation and phase matching conditions require that the radiation co-propagate coherently with the Stokes probe beam with a frequency ω_s, giving rise to the stimulated Raman line and leaving the system in the $|f\rangle\langle f|$ state. The output Stokes field is given by the Maxwell equation

$$\frac{\partial^2 E_s(z,t)}{\partial z^2} - \frac{1}{c^2}\frac{\partial^2 E_s(z,t)}{\partial t^2} = \frac{4\pi}{c^2} N \frac{\partial^2 P}{\partial t^2} \approx \frac{4\pi}{c^2} N\alpha_{fi} \frac{\partial^2 \left(Q^* E_p(z,t)\right)}{\partial t^2} \quad , \tag{3}$$

Where *z* is the direction of propagation, *N* is the number of oscillators per unit volume and *P* is the polarization. Equations (2) and (3) are the central equations for stimulated Raman scattering.

The Raman pump field can be taken to precede the Stokes probe field by a time t_D and both fields have Gaussian pulse envelopes

$$E_p(z,t) = E_p^0 e^{-(t+t_D-z/c)^2/2\tau_p^2} e^{-i\omega_p(t+t_D-z/c)} \tag{4}$$

$$E_s(z,t) = E_s^0 e^{-(t-z/c)^2/2\tau_s^2} e^{-i\omega_S(t-z/c)} \quad . \tag{5}$$

We first solve for $Q(t)$ using equation (2) and the result is then used in the Maxwell equation (3) to solve for the output Stokes field $E_s(z,t)$. The solutions are best carried out in frequency space, giving the output Stokes spectrum

$$E_s(z,\omega) = \left\{1 + i2\pi\chi_R(\omega,t_D)\left|E_p^0\right|^2 \frac{\omega z}{c}\right\} E_s^{free}(z,\omega) \equiv E_s^{free}(z,\omega) + E_{SR}(z,\omega) \tag{6}$$

where $\chi_R(\omega,t_D)$ is the Raman susceptibility

$$\chi_R(\omega,t_D) \equiv N\left(\alpha_0'\right)^2 (2\omega_0)^{-1}(2\pi)^{-1/2}\tau_p e^{-t_D^2/2\tau_p^2} g(\omega,t_D) \tag{7}$$

$$g(\omega,t_D) \equiv -i\sqrt{2\pi}\,\tau_p^{-1}\int_0^\infty e^{i(\omega+\omega_0-\omega_p)t} e^{-(t+t_D)^2/2\tau_p^2 - \gamma t} dt \tag{8}$$

and the free Stokes spectrum is

$$E_s^{free}(z,\omega) = E_s^0\sqrt{2\pi}\tau_s e^{-(\omega-\omega_S)^2\tau_s^2/2} e^{i\omega z/c} \quad . \tag{9}$$

The FSRS measures the Raman gain, $G_R(\omega,t_D)$, given by the ratio of the intensity of the Stokes probe spectrum with and without the presence of the Raman pump,

$$G_R(\omega,t_D) = \frac{\left|E_s(z,\omega)\right|^2}{\left|E_s^{free}(z,\omega)\right|^2} = \left|1 + i2\pi\chi_R(\omega,t_D)\left|E_p^0\right|^2 \frac{\omega z}{c}\right|^2 \tag{10}$$

$$\equiv [1 + A(\omega,t_D)]^2 + [B(\omega,t_D)]^2$$

where

$$A(\omega,t_D) = \kappa e^{-t_D^2/2\tau_p^2}\,\omega\int_0^\infty Cos[(\omega+\omega_0-\omega_p)t] e^{-(t+t_D)^2/2\tau_p^2 - \gamma t} dt \tag{11}$$

$$B(\omega,t_D) = \kappa e^{-t_D^2/2\tau_p^2}\,\omega \int_0^\infty Sin[(\omega+\omega_0-\omega_p)t]e^{-(t+t_D)^2/2\tau_p^2-\gamma t}\,dt \qquad (12)$$

and κ is a collection of constants that can be taken as a parameter to fit the experimental data. The Raman gain is nearly an even function in ω about $(\omega_p-\omega_0)$ and can be easily evaluated numerically to generate a lineshape for any given pulse delay t_D.

Figure 2 illustrates the time-dependent electric fields, $E_p(t)$, $E_s(t)$, coherent vibration, $Q(t)$, total polarization, $P_{Total}(t)$, and output Stokes field, $E_s^{free}(t)+E_{SR}(t)$ relevant to FSRS on the left, and the corresponding power spectra on the right. The high resolution Raman gain spectrum at $(\omega_p-\omega_0)$ can be seen on the right of figure 2(e).

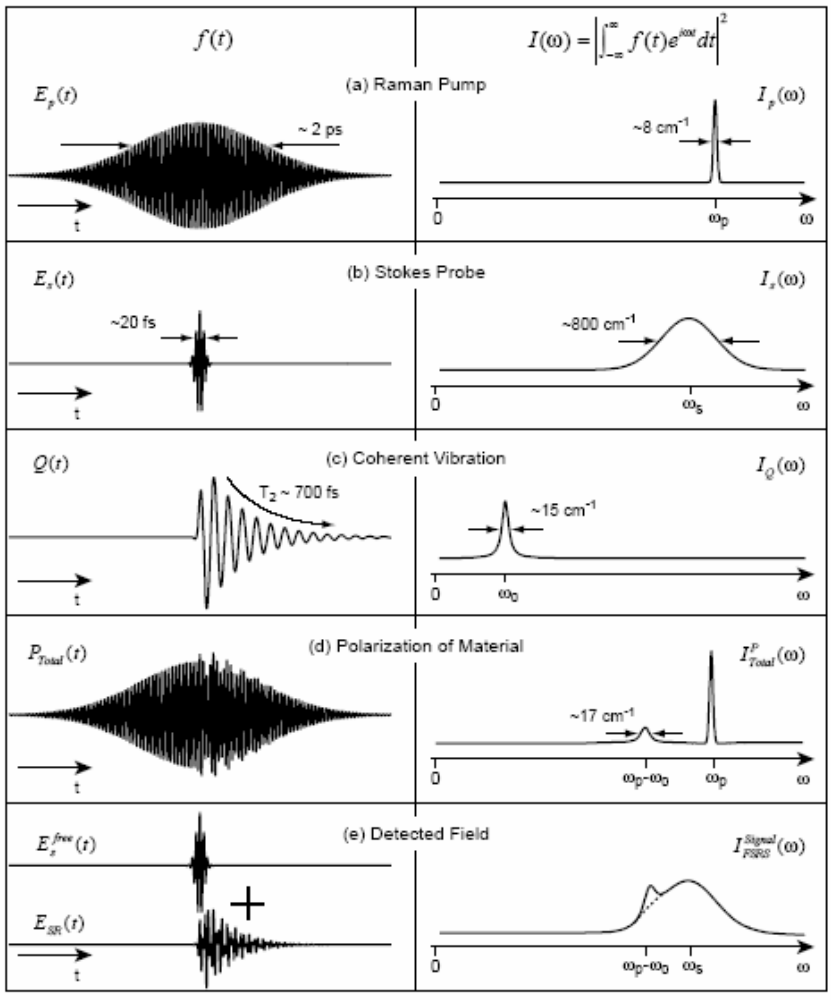

Figure 2. Relevant time-dependent functions and power spectra for FSRS

3. Experimental Results and Discussion

The contour plots of the experimental Raman gain spectra of cyclohexane as a function of the time delay t_D between pulses for the 802 cm^{-1} symmetric C-C stretch and the 1027 cm^{-1} doubly degenerate C-C stretch modes are shown in figure 3(a). The change in the lineshape with time delay is most apparent for the intense 802 cm^{-1} peak, with a similar pattern for the weaker 1027 cm^{-1} band. The spectral line broadens with increasingly positive time delays. As the time delay t_D decreases in the negative direction, the peak becomes narrower and the lineshape develops small Raman loss side wings, denoted by the dotted contour lines, for the 802 cm^{-1} band. The maximum of the Raman gain appears at $t_D \approx -1$ ps, while an initial guess would suggest that the maximum gain occur at t_D = 0 ps when the temporal overlap between the Raman pump and Stokes probe pulse envelopes is the largest. The experimental observations can be modeled using equation (10) with the vibrational dephasing time γ as a fitting parameter. The simulation using γ^{-1} of 2.0 ± 0.2 ps for the 802 cm^{-1} mode and 0.65 ± 0.02 ps for the 1027 cm^{-1}, as shown in figure 3(b), gives the best agreement with the experimental spectra. Elsewhere, using different techniques, Tanabe [9] obtained about 4.8 ps for γ^{-1} of the 802 cm^{-1} mode, and Arndt and McClung [10] reported 0.9 ps for the 1027 cm^{-1} mode.

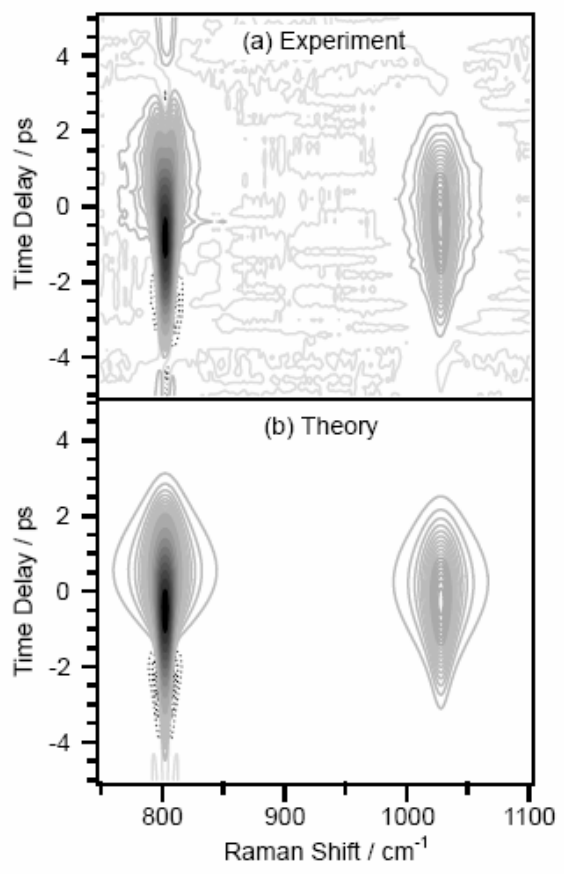

Figure 3. Contour plot of the Raman gain spectra of cyclohexane as a function of time delay t_D: (a) experimental spectra, (b) simulated spectra.

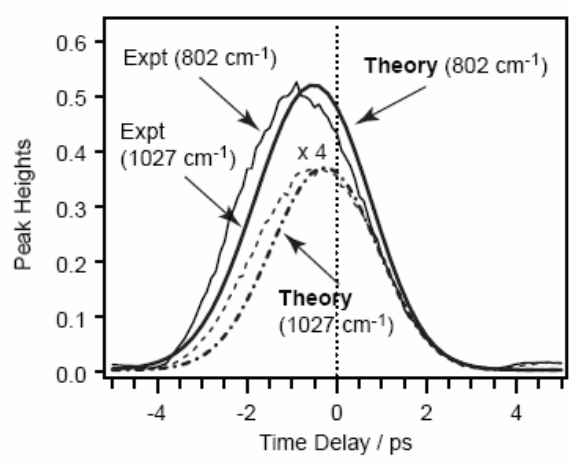

Figure 4. Experimental and theoretical peak intensity of the 802 cm^{-1} and 1027 cm^{-1} bands of cyclohexane as a function of time delay t_D between the Raman pump and Stokes probe pulses.

A comparison of the experimental and theoretical results for the peak Raman gain intensity profile as a function of time delay for the 802 and 1027 cm^{-1} modes is shown in figure 4. The doubly degenerate vibrational mode (1027 cm^{-1}) has a broader bandwidth and reaches the maximum Raman gain at a slightly earlier time delay (-0.7 ps) than the totally symmetric 802 cm^{-1} mode (-1 ps). The theoretical gain profile obtained from the simulation used in figure 3 agrees well with the experimental results. The coupled wave theory can explain why the maximum gain appears at a negative time delay rather than at $t_D = 0$: The polarization that radiates as the stimulated Raman wave is dependent on the product of the coherent vibration $Q^*(z,t)$ and the Raman pump field $E_p(z,t)$, as in equation (3). Although the largest coherent vibration is induced in the sample when the maxima of the Raman pump and Stokes probe are coincident (t_D = 0), the coherent vibration interacts with the Raman pump field for a longer period of time at more negative time delays. Due to these two competing factors, it is not surprising that the maximum gain appears at a slightly negative time delay.

4. Conclusion

The coupled wave theory of FSRS can successfully account for the experimental data on the dependence of the FSRS lineshape on the time delay of the Raman pump and Stokes probe pulses for the two most prominent modes of cyclohexane, 802 and 1027 cm^{-1}, in the ground state. The theoretical simulations provide a good fit to the experimental lineshapes, recovering broad linewidths at positive time delays and narrower linewidths with small Raman loss features on the wings at negative time delays. From the fit, we have determined the vibrational dephasing time of the 802 and the 1027 cm^{-1} modes to be 2.0 ps and 0.65 ps, respectively, and these are likely to be lower bounds. The theoretical prediction of the Raman gain intensity profile with time delay also agrees well with experimental observation, peaking at a slightly negative time delay.

References

[1] Yoshizawa M, Aoki H and Hashimoto H 2001 *Phys. Rev.* B **63** 180301
[2] McCamant D W, Kukura P and Mathies R A 2003 *J. Phys. Chem.* A **107** 8208
[3] McCamant D W, Kukura P and Mathies R A 2003 *Appl. Spectrosc.* **57** 1317
[4] McCamant D W, Kukura P, Yoon S and Mathies R A 2004 *Rev. Sci. Instrum.* **75** 4971
[5] Shen Y R 1984 *The Principles of Nonlinear Optics* (New York: Wiley)
[6] Lee S Y, Zhang D, McCamant D W, Kukura P and Mathies R A 2004 *J. Chem. Phys.* **121** 2632
[7] Yoon S, McCamant D W, Kukura P, Mathies R A, Zhang D and Lee S Y 2005 *J. Chem. Phys.* **122** 024505
[8] Lee D and Albrecht A C 1985 A unified view of Raman, resonance Raman, and Fluoresence Spectroscopy (and their analogues in two-photon absorption) *Advances in Infrared and Raman Spectroscopy* eds Clark R J H and Hester R E (Heyden: Wiley) chapter 4 pp 179-213
[9] Tanabe K 1981 *Chem. Phys. Lett.* **83** 397
Tanabe K 1982 *J. Chem. Phys.* **86** 319
[10] Arndt R and McClung R E D 1979 *J. Chem. Phys.* **70** 5598